Inherited retinal degenerations: clinical characterization on the road to therapy

Talib, M.

5.
LRAT-associated retinal dystrophies

5.1

Long-term follow-up of retinal degenerations associated with *LRAT* mutations and their comparability to phenotypes associated with *RPE65* mutations

Mays Talib, MD[1], Mary J. van Schooneveld, MD, PhD[2], Roos J.G. van Duuren, MD[1], Caroline Van Cauwenbergh, PhD [3,4], Jacoline B. ten Brink, BAS[5], Elfride De Baere, MD, PhD[4], Ralph J. Florijn, PhD[5], Nicoline E. Schalij-Delfos, MD, PhD[1], Bart P. Leroy, MD, PhD[3,4,6], Arthur A. Bergen, PhD[5,7], Camiel J.F. Boon, MD, PhD[1,2]

Transl Vis Sci Technol 2019;8(4):24

1 Department of Ophthalmology, Leiden University Medical Center, Leiden, The Netherlands.
2 Department of Ophthalmology, Academic Medical Center, Amsterdam, The Netherlands.
3 Department of Ophthalmology, Ghent University and Ghent University Hospital, Ghent, Belgium.
4 Center for Medical Genetics, Ghent University and Ghent University Hospital, Ghent, Belgium.
5 Department of Clinical Genetics, Academic Medical Center, Amsterdam, The Netherlands.
6 Ophthalmic Genetics & Visual Electrophysiology, Division of Ophthalmology, The Children's Hospital of Philadelphia, Philadelphia, Pennsylvania, USA.
7 The Netherlands Institute for Neuroscience (NIN-KNAW), Amsterdam, The Netherlands.

ABSTRACT

Purpose: To investigate the natural history in patients with *LRAT*-associated retinal degenerations (RDs), in the advent of clinical trials testing treatment options.

Methods: A retrospective cohort of 13 patients with *LRAT*-RDs.

Results: Twelve patients from a genetic isolate carried a homozygous c.12del mutation. One unrelated patient carried a homozygous c.326G>T mutation. The mean follow-up time was 25.3 years (SD 15.2; range 4.8-53.5). The first symptom was nyctalopia (n = 11), central vision loss (n = 1), or light-gazing (n = 1), and was noticed in the first decade of life. Seven patients (54%) reached low vision (visual acuity < 20/67), four of whom reaching blindness (visual acuity < 20/400), respectively, at mean ages of 49.9 (SE 5.4) and 59.9 (SE 3.1) years. The fundus appearance was variable. Retinal white dots were seen in six patients (46%). Full-field electroretinograms (n = 11) were nondetectable (n = 2; ages 31-60), reduced in a nonspecified pattern (n = 2; ages 11-54), or showed rod-cone (n = 6; ages 38-48) or cone-rod (n = 1; age 29) dysfunction. Optical coherence tomography (n = 4) showed retinal thinning but relative preservation of the (para-)foveal outer retinal layers in the second (n = 1) and sixth decade of life (n = 2), and profound chorioretinal degeneration from the eighth decade of life (n = 1).

Conclusions: *LRAT*-associated phenotypes in this cohort were variable and unusual, but generally milder than those seen in *RPE65*-associated disease, and may be particularly amenable to treatment. The window of therapeutic opportunity can be extended in patients with a mild phenotype.

Translational relevance: Knowledge of the natural history of *LRAT*-RDs is essential in determining the window of opportunity in ongoing and future clinical trials for novel therapeutic options.

INTRODUCTION

Inherited retinal degenerations (IRD) comprise a collection of heterogeneous diseases characterized by variable progressive dysfunction of rods and/or cones. Leber congenital amaurosis (LCA) is the most severe IRD, characterized by severe visual impairment, nondetectable rod and cone function in the first year of life, and often nystagmus. Retinitis pigmentosa (RP) or rod-cone degeneration, the most common IRD, is characterized by progressive nyctalopia, (mid)peripheral visual field constriction, and finally, loss of central vision.[1] Pathogenic variants in several genes that are typically associated with LCA, can also cause RP.[2]

Genes that are mutated in IRDs encode proteins that function through multiple mechanisms and pathways involving structural and functional retinal integrity, such as the retinoid cycle.[3] This cycle regenerates the visual pigments that are used after light activation. Key enzymes in the retinoid cycle are retinal pigment epithelium (RPE)-specific protein 65 kDa (RPE65) and lecithin:retinol acetyltransferase (LRAT), which are encoded by the *RPE65* and *LRAT* gene, respectively. Photoactivation induces the configurational change of the visual chromophore 11-*cis*-retinal into all-*trans* retinal in the photoreceptor, and the subsequent reduction to all-*trans* retinol. The released all-*trans*-retinol is shuttled to the RPE cells, and esterified to all-*trans*-retinyl esters by the LRAT enzyme, providing the substrate for the RPE65 enzyme. Ultimately, 11-*cis* retinal is resupplied to the photoreceptors. LRAT and RPE65 are thus essential enzymes in the regeneration of functional visual pigment, and a deficiency of either enzyme leads to an impairment in the visual cycle.[4, 5] Mutations in *RPE65* have been associated with several severe IRDs in the autosomal recessive form, causing 6% to 8% of LCA cases, and 5% of cases of childhood-onset RP.[6-15] Rarely, cases of autosomal-dominant IRD have been described in association with mutations in *RPE65*.[16-18] Although reports on the phenotype associated with *LRAT* mutations are scarce, case reports and small case series have shown an association with LCA and childhood-onset RP.[19-23] *LRAT* mutations have been predicted to cause less than 1% of these cases.[6]

While no established and effective treatment is available for most IRDs, the advent of subretinal gene therapy in the treatment of LCA and RP associated with *RPE65* mutations and the favorable results have recently led to the first approval of subretinal gene therapy by the US Food and Drug Administration, and provide a promising perspective for related disorders.[24-26] A trial investigating the safety and efficacy of oral 9-*cis*-retinal supplementation has shown promising results in the treatment of IRDs associated with mutations in *RPE65* and *LRAT*, combining these two patient groups.[27,24] However, due to the rarity of IRDs associated with *LRAT* mutations, little is known about the associated phenotypic spectrum, and the degree of clinical resemblance to phenotypes associated with *RPE65* mutations.

The purpose of this study was to provide a description of the initial and longitudinal clinical characteristics of patients with IRDs associated with *LRAT* mutations, and to compare these findings with previously reported clinical characteristics of IRDs associated with *RPE65* mutations.

METHODS

Patient population and genetic analysis

Patients with bi-allelic molecularly confirmed pathogenic variants in *LRAT* were collected from the database for hereditary eye diseases (Delleman archive) at the Academic Medical Center (AMC) in Amsterdam, resulting in a cohort of 12 patients from a Dutch genetic isolate. One Turkish-Belgian patient (Turkish descent) was included from Ghent University Hospital, Belgium. Informed consent was obtained from Dutch patients in this study, and the study adhered to the tenets of the Declaration of Helsinki. For the Belgian patient, informed consent for this retrospective study was waivered by the Ethics Committee of Ghent University Hospital. Mutational analyses for Dutch patients were performed at the AMC, and at the Ghent University Hospital for the Belgian patient. In the Dutch patients, no pathogenic variants were found with the autosomal recessive RP chip (version 2011/2012; Asper Biotech,Tartu, Estonia), which included *RPE65*, but sequence analysis of *LRAT* revealed a previously described homozygous frameshift mutation,[28] which led to a premature stop codon (c.12del; p.[Met5Cysfs*53]; NM_004744.4), and segregated with the disease. Because the Dutch patients originated from the same genetic isolate as the previously described *CRB1*-RP cohorts,[29, 30] the presence of bi-allelic *CRB1* mutations was excluded in all patients. The Turkish-Belgian patient carried a homozygous missense mutation in *LRAT* (c.326G>T; p.[Arg109Leu]), found through identity by descent-guided Sanger sequencing,[31] and a heterozygous rare variant in *CRB1* (c.4060G>A; p.[Ala1354Thr]), found with LCA chip analysis. Sanger sequencing of the coding regions and intron-exon borders revealed no second *CRB1* mutation.

Clinical assessment and data collection

Through a standardized medical records review, data on initial symptoms, best-corrected visual acuity (BCVA), refractive error, slit-lamp biomicroscopy of the anterior segment, and dilated fundus examination were obtained for all patients. International Society for Clinical Electrophysiology of Vision standard full-field electroretinography (ERG) results and data on color vision testing were available for 11 patients (Ishihara in all patients; Farnsworth D-15 dichotomous color blindness test, Roth 28-hue desaturated test, and Hardy-Rand-Rittler plates in a subset).[32] Goldmann visual fields (GVFs) were performed in six patients. Fundus photographs were available for 11 patients, and spectral-domain optical coherence tomography (SD-OCT) with Heidelberg Spectrals (Heidelberg Engineering, Heidelberg, Germany) was available for four patients. Thirty-degree fundus autofluorescence images (FAF; Heidelberg Engineering) were available for three patients.

Statistical analysis

Data were analyzed using SPSS version 23.0 (IBM Corp, Armonk, NY). Kaplan Meier's methodology was used to analyze the time-to-event for low vision (BCVA < 20/67) and blindness (BCVA < 20/400), based on the World Health Organization criteria, using the better-seeing eye. GVF areas of the V4e target were digitized and converted to seeing retinal areas in millimeters squared using a method described by Dagnelie.[33] *P* values < 0.05 were considered statistically significant.

RESULTS

Of 13 subjects, seven were male. The mean age at first examination was 24.4 years (SD 15; range 1.6-53.6 years). The mean follow-up time was 25.3 years (SD 15.2; range 4.8-53.5 years), with a mean number of 9.5 visits per patient (SD 6.4; range 5-26). Symptoms started as early as the first decade of life in all patients (Table 1), but the 12 patients from the genetic isolate reported a slow progression. Nine patients (69%) first started using visual aids other than glasses between the ages of 29 and 43. A comparison of the phenotypes associated with mutations in *LRAT* and *RPE65* is provided in Table 2.

Ophthalmic and fundoscopic features

The mean spherical equivalent of the refractive error (SER) was +2.2 diopters (D; SD 2.1; range -2.4D to +4.7D), and all but two patients (85%) were mildly (+1D ≤ SER < +3D; n = 6) or moderately (+3D ≤ SER < +6D; n = 5) hyperopic. Hyperopic patients were aged 17 to 59 years, and nonhyperopic patients were aged 11 and 13 years at the time of initial examination of the SER. Nuclear (n = 2) or posterior subcapsular (n = 2) cataract was observed in four patients. Two patients underwent uncomplicated cataract surgery in their seventh decade of life.

Abnormalities in the vitreous were present in 10 of 13 patients (77%), all from the genetic isolate, and consisted of cells or dust-like particles (n = 6), veils (n = 6), or synchysis scintillans (n = 2).
All patients from the genetic isolate had optic disc pallor and vascular attenuation, and 11 of 13 patients (85%) had peripapillary chorioretinal atrophy, varying from a small to moderately sized (n = 2) or large (n = 1) but distinct atrophic border, to a large atrophic zone encompassing both the peripapillary region and parts of the posterior pole (n = 8). Bone-spicule-like pigment migration in the (mid)periphery was first seen at the mean age of 44.6 years (SD 8.8; range 31.5-55.2) in all but two patients aged 17.0 and 20.9 years at the last examination, but intraretinal pigmentation remained sparse in three patients (23%). Eight patients (62%) from the genetic isolate had sharply demarcated areas of atrophic depigmentation in the periphery (Table 1). White dots were seen in the (mid)periphery in six patients (46%) aged 17 to 64 years, including the Turkish-Belgian patient. Considerable intrafamilial variability was observed (Figure 2). Macular RPE involvement ranged from mild RPE alterations (n = 7), first described at a mean age of 39.8 years (SD 17.0;

range 11.7-59.4), to profound atrophy of the posterior pole and the central macula (n = 4), first described at a mean age of 42.6 (SD 20.5; range 22.1-68.3). The macular RPE had a normal aspect in two patients aged 17.0, and 55.2 years.

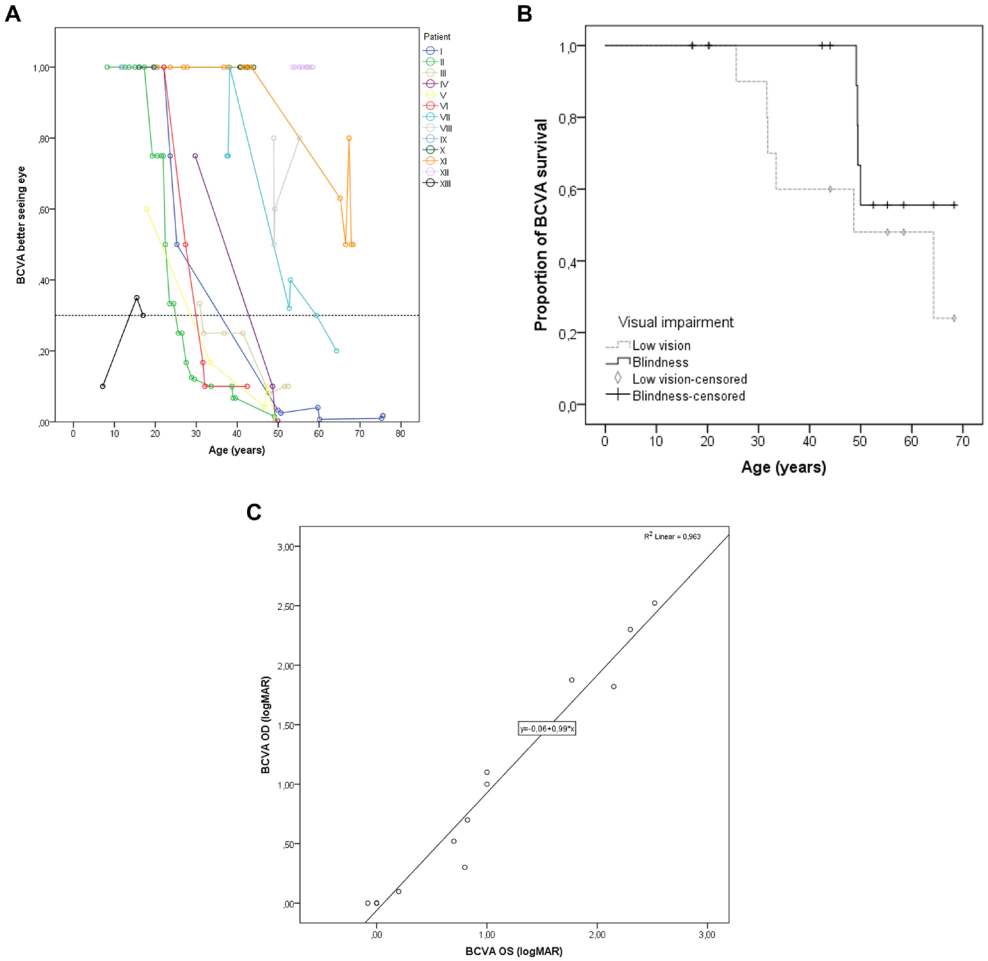

Figure 1. Visual acuities in patients with *LRAT*-associated retinal degeneration. A. The course of decline of the best-corrected visual acuity (BCVA) in individual patients. For illustrative purposes, a BCVA of 20/20 was considered the ceiling, also in patients with a BCVA > 20/20. The dashed line indicates the cutoff value for low vision (20/67), based on the World Health Organization criteria. The individual line for patient XII, the only patient not from the genetic isolate, is shown in black. **B.** Kaplan-Meier plots showing the proportion of patients with a BCVA above low vision (BCVA ≥ 20/67) and above blindness (BCVA ≥ 20/400). Censored observations (i.e. patients who had not reached low vision or blindness at the last follow-up moment) are depicted as vertical bars (blindness) or rhombi (low vision). The median age for reaching low vision was 48.6 years (standard error 14.1). The median age for reaching blindness could not be calculated, as fewer than 50% of subjects became blind during follow-up. **C.** The relation of the BCVA in logarithm of the minimum angle of resolution (logMAR) between the right and left eye at the last clinical visit, showing a linear relationship.

Table 1. Clinical characteristics of patients with *LRAT*-associated retinal degeneration

		Symptoms (DOL at onset)*				Fundus		
ID	Sex, Age (y)	Nyctalopia	VF loss	VA loss	BCVA	Macula	(Mid)periphery	ERG (Age)†
I	M, 75‡	+ (1st)	+ (3rd)	+ (2nd)	CF	Profound chorioretinal and RPE atrophy, sharply demarcated. Pigment clumping.	Bone spicule pigmentation, RPE mottling and depigmentation spots. No white-yellow dots.	ND (52)
II	M, 49‡	+ (infancy)	+ (1st)	+ (1st)	CF	Sheen, RPE alterations	Extensive bone spicule pigmentation, RPE atrophy. Extensive white-yellow dots.	CRD (28)
III	F, 52	+ (infancy)	+ (3rd)	+ (3rd)	20/200	Retinal and RPE atrophy.	Bone spicule pigmentations, extensive clumping in atrophic supra-temporal region, coarse salt and pepper. No white dots, but hypo-pigmented dots. Paving stone-like degeneration.	ND (30)
IV	M, 49	+ (infancy)	+ (3rd)	+ (2nd)	CF	RPE alterations, choroidal atrophy.	Bone spicule pigmentations, extensive pigment clumping. Salt and pepper. Paving stone-like degeneration in far periphery. RPE mottling. No white-yellow dots.	MR (31)
V	F, 49	+ (infancy)	+ (2nd)	+ (2nd /3rd)	CF	Sheen, RPE atrophic alterations	Extensive bone spicule and coarse pigmentation. Salt and pepper. RPE mottling. Paving stone-like atrophic depigmentation.	NA
VI	M, 42	+ (infancy)	+ (3rd)	+ (2nd)	20/200	Chorioretinal and RPE atrophy spanning posterior pole and beyond vascular arcade.	Bone spicule and coarse pigmentation. RPE mottling. Choroid atrophy. No white dots or paving stone degeneration.	NA
VII	F, 64	+ (infancy)	+ (3rd)	+ (<4th)	20/100	Difficult to assess due to synchysis scintillans. Small pigmentations.	Bone spicule pigmentation. RPE mottling. Paving stone-like degenerative depigmentation. White dots, which were no longer observed at the age of 59 onward, after they had been repeatedly observed between the ages of 34-52.	RCD (37)
VIII	M, 55	+ (1st)	+ (<5th)	+ (1st)	20/25	Sheen, RPE atrophy around spared fovea.	Few bone spicule pigmentations. RPE mottling, lobular atrophy. White-yellow dots in far periphery.	RCD (49)
IX	M, 20	+ (1st)	+ (1st)	-	20/20	Sheen, normal pigmentation, white dots.	Salt and pepper. RPE mottling. Drusen. White-yellow dots.	RCD (16)

Table 1. Continued

X	F, 44	+ (1st)	+ (2nd)	+ (2nd)	20/20	No sheen, subtle white dots on a pale retina, subtle granular RPE changes.	Bone spicule pigmentations. Patches of paving stone-like retinal and RPE atrophy, RPE mottling. White yellow dots. Retina generally hypo-pigmented.	RCD (40)
XI	F, 68	+ (infancy)	+ (5th)	-	20/40	Atrophic RPE alterations.	Choroideremia-like atrophic zones with relatively little bone spicule pigmentation. Paving stone-like degeneration.	RCD (42)
XII	F, 58	+ (infancy)	-	-	20/16	RPE alterations.	Few clustered bone-spicule and nummular pigmentations, mainly inferiorly. Midperipheral chorioretinal atrophy.	RR (53)
XIII	M, 17	+ (infancy)	+*	+ (1st)	20/66	Central macula with normal appearance, white dots in the superior posterior pole.	Outer retinal atrophy, no intra-retinal hyperpigmentation, white-greyish dots	RCD (1)

CRD, cone-rod degeneration pattern; DOL, decade of life; ERG, electroretinography; ND, nondetectable; MR, minimal response; NA, data not available; ND, no detectable amplitudes; RCD, rod-cone degeneration pattern; RR, reduced response, pattern not specified; VA, visual acuity; VF, visual field.

* The decade of life during which the patient started noticing the symptom is shown between parentheses. Mild adult-onset nystagmus was documented in patients I, II, and X, starting from the fifth decade of life. In patient XIII, light-gazing and nystagmus were noticed by the parents during the first months of life. Subjective visual field complaints were not documented, but there was concentric constriction on Goldmann kinetic perimetry in the second decade of life. Photopsias were reported in 7/13 patients (54%).

† Full-field ERGs were not performed at the last clinical visit, but the results of the initial ERG are shown, and the age at the time of ERG examination is shown in parentheses. In patients II and VIII, later ERGs showed nondetectable dark- and light-adapted, at the ages of 49 and 55 years, respectively. In the Turkish-Belgian patient, patient XIII, dark-adapted responses were nondetectable, with severely diminished light-adapted responses (<5 μV), leading to a diagnosis of early-onset panretinal degeneration.

‡ These patients are siblings.

Central visual function

The median initial BCVA was 20/20 (IQR in decimals 0.33; range 20/100-20/20), at a median age of 20.6 years (IQR 20.3; range 7.2-53.6 years). Figure 1 illustrates a better preservation of the BCVA in patients from the genetic isolate than in patient XIII, the youngest patient (aged 17 at the final visit), who was Turkish-Belgian. Survival analysis revealed no BCVA-based visual impairment until the third decade of life (Figures 1A, 1B). The mean ages for reaching low vision and blindness were 49.9 (SE 5.4; 95% CI 39.3-60.5) and 59.9 years (SE 3.1; 95% CI 53.8-66.0), respectively, with seven patients (54%) reaching low vision in the better seeing eye during the follow-up period, four of whom (31%) reaching blindness. Five patients (38%) maintained a BCVA of 20/40 or more into the third to seventh decades of life (BCVA > 20/25 in four patients), while patient XIII had a BCVA of 20/66 at the final visit. Spearman's rank correlation coefficients showed a high degree of intraindividual between-eye symmetry in BCVA at the first (0.78; $p = 0.002$) and last (0.98; $p < 0.00001$) visit.

Color vision testing in 11 patients (10 from the genetic isolate) showed a severe or near-complete deficiency in all axes in eight patients aged 15.5-59.4 (patients I, III, V-IX, XIII), or multiple errors in different axes in three patients aged 12.6-43.1 (patient II: protan; patient X and XI: tetartan and tritan; patient XI also deutan), despite a nonimpaired concurrent BCVA in seven of 11 cases.

Visual fields and electroretinography

Visual fields were recorded in 10 patients (Supplementary Table S1), using different modalities (GVF in six subjects). Visual fields predominantly showed peripheral constriction or midperipheral scotomas with relative preservation of central vision in seven of 10 patients (70%), and a central scotoma in three of 10 patients (30%) including two brothers (Supplementary Figure S1). Initial seeing retinal areas for the V4e target were large (>250 mm^2) in all patients, aged 15.5 to 48.9 years at the time of examination, with a median of 714.3 mm^2 (IQR 123.9; range 482.1-774.2). During follow-up, visual field-based low vision (central diameter <20°) or blindness (central diameter <10°) was observed in two patients from the genetic isolate at the ages of 23.6 (patient I) and 54.1 years (patient XII), despite a normal concurrent BCVA (Table 2). Patient I reached visual field-based blindness 26 years before reaching BCVA-based blindness. The degree of between-eye symmetry of seeing retinal areas was high (Spearman's rank correlation coefficient 0.89; $p = 0.019$).

Initial ERG examination showed a rod-cone pattern (n = 5; ages 37.6-49.0 in the genetic isolate; second year of life in patient XIII), cone-rod pattern (n = 1; age 28.9), severely reduced responses in a nonspecified pattern (n = 3; ages 11.9-53.6), or a nondetectable response (n = 2; ages 30.8-52.1 years). Later ERGs showed progression to nondetectable responses in two more patients in their fifth to sixth decades of life.

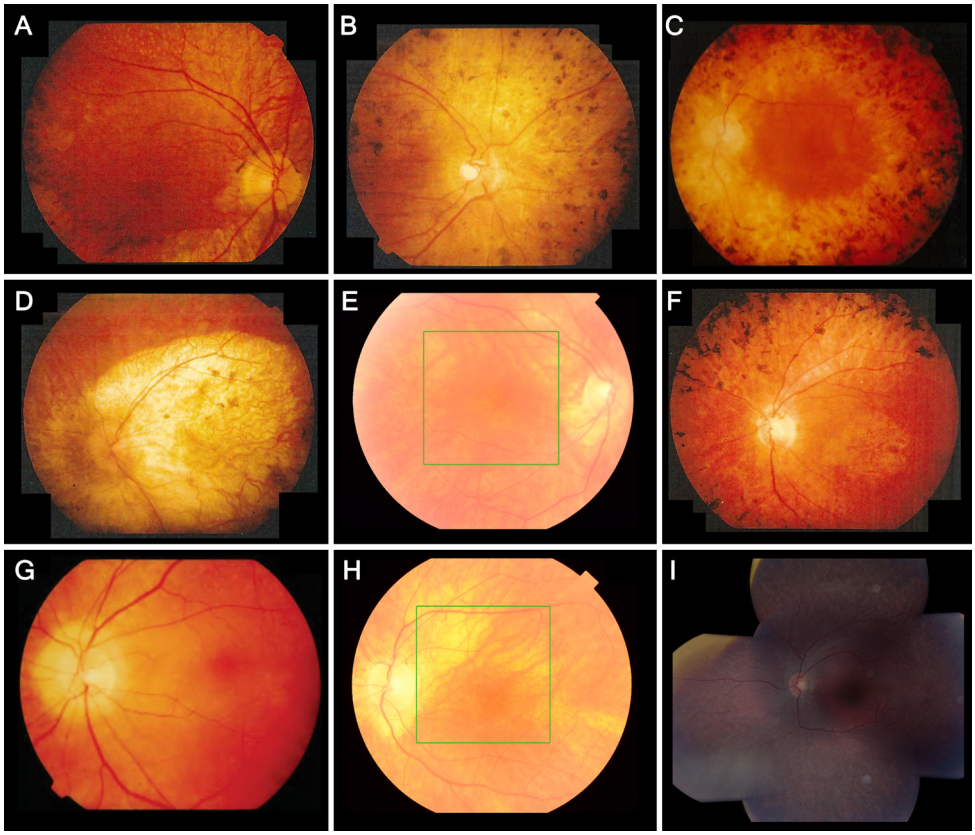

Figure 2. Fundus photographs showing retinal features and intrafamilial variability in patients with *LRAT*-associated retinal degeneration. Reported ages are at the time of fundus photography. **A.** Patient II, aged 39, showing pigmentary changes in the posterior pole, a macular sheen, and yellow-white dots, associated with retinitis punctata albescens, in the midperiphery. The periphery, not shown here, showed extensive bone spicule hyperpigmentation. **B.** Patient IV, aged 49, showing a pale optic disc, peripapillary atrophy, vascular attenuation, mottled retinal pigmentary epithelium (RPE) changes and clumping in the posterior pole, and atrophy in the nasal midperiphery. In the inferior midperiphery, not shown here, paving stone-like atrophic zones were seen with fundoscopy. **C.** Patient VI, aged 42, showing retinal atrophy, and widespread bone spicule-like and coarse hyperpigmentation extending into the posterior pole. The central macula is relatively spared, with mild RPE alterations. **D.** Patient I, aged 50, showed profound chorioretinal atrophy of the posterior pole and along the vascular arcade. The periphery, not shown here, showed mild RPE mottling, several paving stone-like degenerations, and little bone spicule-like hyperpigmentation. **E.** Patient XII, aged 56, showing peripapillary atrophy and areas of retinal thinning along the superior vascular arcade, with no RPE changes in the central retina. In the inferonasal mid-periphery, not shown here, a few round and bone spicule-like pigmentations were clustered. **F.** Patient V, aged 47, showed atrophic RPE alterations and a sheen in the central macula, atrophy around the optic disc and along the vascular arcade, and extensive bone spicule-like pigmentation in the midperipheral retina. **G-H.** Patient XI, showing the disease progression between the ages of 43 (**G**) and 67 (**H**). At the age of 43, this patient showed peripapillary atrophy, yellow-white dots below the superior vascular arcade, and no RPE changes of the central macula. At the age of 67, the white dots were no longer visible, and the posterior pole showed zones of atrophic RPE. **I.** Composite fundus photography of the left eye of patient XIII at the age of 15, showing peripapillary atrophy, a normal macula, limited intraretinal white dots in the superior macula

that appear less brightly yellow and less sharply circumscribed than the white-yellow dots seen in patients from the genetic isolate, and fleck-like outer retinal atrophy in the (mid-)periphery.

Findings on retinal imaging

SD-OCT scans of four patients (I, XI, XII, and XIII) showed outer retinal attenuation in the peripheral macula and a relatively well-preserved foveal and parafoveal outer retina in patient XIII during his second decade of life, and in patient XII until her sixth to seventh decades of life. Patient XI showed progressive thinning of the outer nuclear layer and hyperreflective outer retinal bands in her seventh decade of life (Figures 3D, 3F). In the mildly hyperopic patient I, an SD-OCT scan at the age of 76.5 showed a markedly thinned choroid, and generalized outer retinal atrophy (Figures 3G-I). FAF images in three patients showed granular or mottled hypo-autofluorescence and a hyperautofluorescent ring in two patients from the genetic isolate (Figures 3B, 3E).

Table 2. Overview of the current literature of *RPE65*- and *LRAT*-associated phenotypes

Phenotype	Additional features	*RPE65*	*LRAT*
IRD*		Biswas et al., 2017[34]	
LCA		Katagiri et al., 2016[10] Srilekha et al., 2015[11] Jakobsson et al., 2014[12] Chen et al., 2013[13] Roman et al., 2013[14] Xu et al., 2012[35] McKibbin et al., 2010[15] Pasadhika et al., 2010[36] Walia et al., 2010[37] Li et al., 2009[38] Simonelli et al., 2007[9] Jacobson et al., 2005;[39] 2008[40] Galvin et al., 2005[41] Booij et al., 2005[2] Silva et al., 2004[42] Hanein et al., 2004[7] Sitorus et al., 2003[43] Hamel et al., 2001[44] Dharmaraj et al., 2000[45]	Den Hollander et al., 2007[20] Sénéchal et al., 2006[22]
Autosomal recessive RP		Chebil et al., 2016 (French)[46] Walia et al 2010[37] Booij et al., 2005[2] Hamel et al., 2001[44] Morimura et al., 1998[47]	Preising et al., 2007 (German)[23] This study
Autosomal dominant IRD	Extensive chorioretinal atrophy	Hull et al., 2016*[16] Bowne et al., 2011[17] (RP)	-
	AVMD/foveal vitelliform lestions	Hull et al., 2016[16]	-

Table 2. Continued

EORD		Hull et al., 2016[16] Kabir et al., 2013[48] El Matri et al., 2006[49] Thompson et al., 2000[50]	Coppieters et al., 2014[31] Dev Borman et al., 2012[21]
EOSRD/ SECORD	Better visual functions than typically seen in LCA	Mo et al., 2014[51] Weleber et al., 2011[52] Lorenz et al., 2008[53] Preising et al., 2007 (German)[23] Paunescu et al., 2005[54] Lorenz et al., 2004[55] Yzer et al., 2003[56] Felius et al., 2002[57]	Thompson et al., 2001[19]
RPA	White-yellow dots		Littink et al., 2012[28] This study
FA	White-yellow dots	Katagiri et al., 2018[58] (flecks) Yang et al., 2017[59] Schatz et al., 2011[60]	
Early and prominent severe cone involvement		Jakobsson et al., 2014[12] (severe visual impairment in childhood)	
Cone-rod dystrophy			This study (good initial visual function; low vision in third decade of life)

AVMD, adult onset vitelliform macular dystrophy; EORD, early onset retinal dystrophy; EOSRD, early onset severe retinal dystrophy; FA, fundus albipunctatus; IRD, inherited retinal dystrophy; LCA, Leber's congenital amaurosis; RP, retinitis pigmentosa; RPA, retinitis punctata albescens; SECORD, severe early childhood onset retinal dystrophy.
* Retinal dystrophy, not otherwise specified.

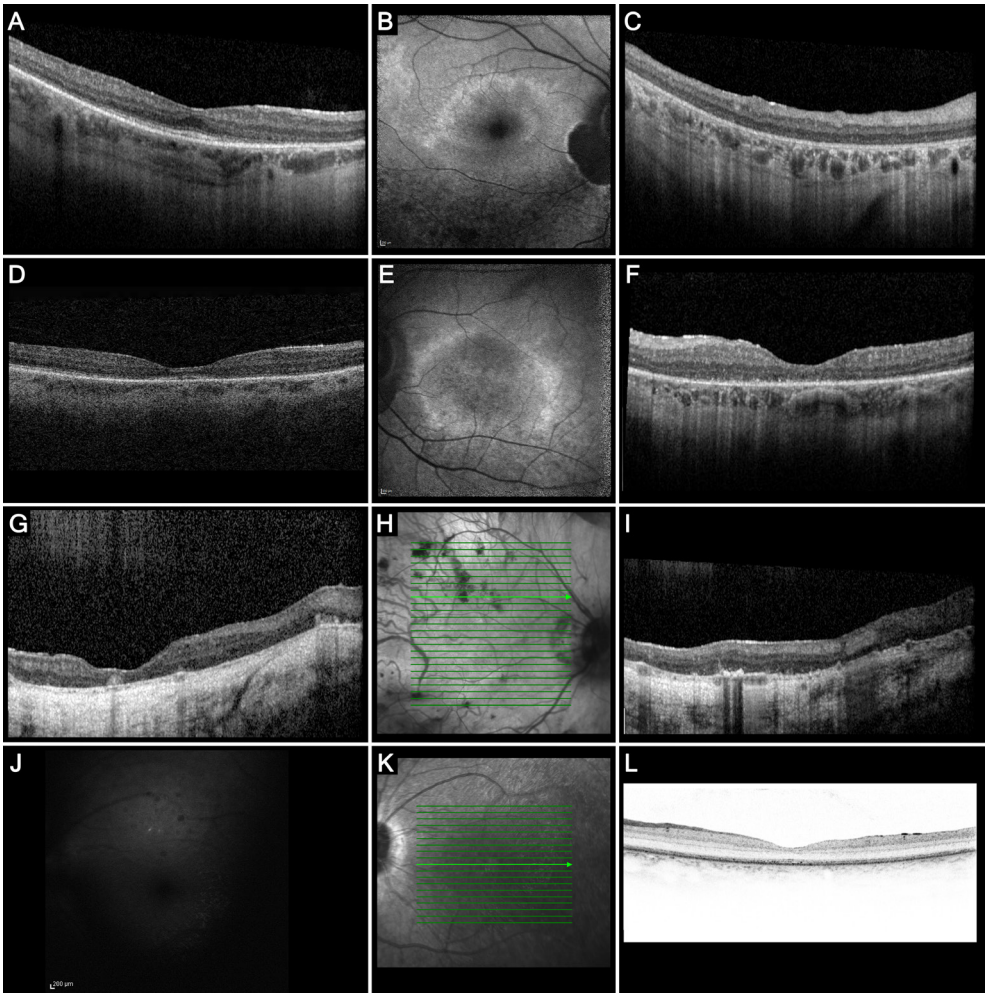

Figure 3. Imaging findings in patients with *LRAT*-associated retinal degeneration. A-C. Imaging in patient XII, aged 57 at the time of examination. Repeated SD-OCT scans between the ages of 54 and 58 showed relative foveal, parafoveal, and temporal perifoveal preservation of the outer nuclear layer and the external limiting membrane (ELM) and ellipsoid zone (EZ), although these hyperreflective outer retinal bands showed a few interruptions, with profound nasal thinning and near-complete disappearance of these layers in areas corresponding with atrophy on the fundus photograph. Follow-up SD-OCT scans over the course of 4 years showed mildly increased outer retinal thinning, mainly in the nasal peri- and parafoveal region. The transition zone between relatively spared outer retina and markedly thinned outer retina colocalized with the hyperautofluorescent ring on FAF (**B**), which also showed a juxtapapillary patch of absent AF, sharply demarcated by a hyper-AF border. Along the inferior vascular arcade, a zone of dense granular hypo-AF was visible. On SD-OCT of the peripheral macula (**C**), small hyperreflective foci with no shadowing were visible in the inner plexiform layer and the inner nuclear layer. To a milder degree, these hyperreflective foci are also visible in (**A**). **D-F.** SD-OCT scan of the right eye of Patient XI at the age of 65 years (**D**), showing a mild epiretinal membrane, and generalized outer retinal thinning and attenuation of the outer retinal hyperreflective bands that was more pronounced at the parafovea, with relative preservation more temporally and at the fovea. FAF imaging of the left eye at the age of 68 (**E**) showed peripapillary atrophy, and a perimacular hyper-AF

ring with mottled hypo-AF inside and outside this hyper-AF ring. The corresponding SD-OCT scan of the left eye (**F**) showed more pronounced outer retinal atrophy, and severe granulation of the EZ band. **G-I.** Patient I, aged 75, showing generalized severe atrophy of the outer nuclear layer, ELM, and EZ, a markedly thin choroid and a scleral tunnel. Large hyperreflective outer retinal accumulations above the RPE level were visible. No concurrent fundus photograph was made in order to attempt to colocalize these accumulations to a funduscopic structure, but earlier fundus photographs taken at the age of 52 (Figure 2D) showed profound atrophy of the retina inside and around the posterior pole. **J-L.** FAF imaging (**J**) of patient XIII at the age of 15 years, carrying a homozygous c.326G>T mutation, showing reduced image quality due to the nystagmus, and a generalized reduced AF with small hypo-AF spots in the posterior pole. No corresponding SD-OCT scan was available at that age, but an SD-OCT scan at the age of 17 years (**K-L**) showed no evident outer retinal thinning, but a granular appearance of the EZ and ELM, with relative preservation of the foveal structure.

DISCUSSION

In this retrospective cohort study of 13 patients with IRDs associated with *LRAT* mutations, we describe the long-term natural history of an unusually mild, albeit variable, phenotype, adding to the phenotypic spectrum of IRDs associated with *LRAT* mutations, and providing further insight regarding the window of opportunity for novel therapeutic strategies.[27, 61] We describe, to the best of our knowledge, the largest cohort to date of patients with IRDs associated with *LRAT* mutations.

While the presentation of the first symptom, usually nyctalopia, was within the first years of life, the retinal phenotypes and the natural disease course reflect a phenotypic variability in IRDs associated with *LRAT* mutations, even within the genetic isolate. Although little is known on the phenotype associated with *LRAT* mutations, due to its rarity, it has been associated with Leber congenital amaurosis and other types of severe early-onset retinal degeneration.[19, 20, 22] In contrast to earlier reports of visual impairment in childhood or adolescence,[20, 27] the mean ages for reaching low vision and blindness in the current cohort were 49.9 and 59.9 years, respectively, with five patients maintaining good BCVA until the final examination, in their third to seventh decade of life. In the Turkish-Belgian patient, symptomatology and visual function were evidently worse, with a BCVA less than 20/40 from the first decade of life, although he had not yet reached low vision at the final visit at the age of 17 years. An earlier study of retinitis punctata albescens included four Dutch patients with the same homozygous frameshift mutation in *LRAT* found in the genetic isolate in this cohort, who had relatively well-preserved BCVA and visual fields compared with patients with retinitis punctata albescens associated with other genes involved in the retinoid cycle, although the patients with *LRAT* mutations described in the previous study were younger (ages 7-19 years) than the patients in the current cohort.[28] In this study, color vision testing was markedly abnormal before BCVA started to decrease. Peripheral visual fields showed more variability, but were relatively well-preserved until the sixth decade of life, with most patients showing relative or absolute concentric constriction with a relatively large central residue, with or without (para)central scotomas. In contrast to these findings, previous reports on *LRAT*-RDs

have lacked quantitative visual field analysis, but where reported, visual field sizes were usually small (<25 mm^2) or intermediate (25-250 mm^2) in the second to third decades of life, with few exceptions,[27] or were reported as severely reduced,[19, 20] with variably sized peripheral crescents of vision.[21]

In gene- or cell-based therapeutic trials that are designed to compare the visual and retinal function between the treated and nontreated control eye, between-eye symmetry is an important assumption. Our findings in this cohort show a high degree of symmetry between affected eyes of the same individual in BCVA and seeing retinal area.

Marked intrafamilial variability was observed in the genetic isolate, with phenotypes varying from cone-rod to rod-cone patterns. This variability was most notable upon ophthalmoscopy, with some patients showing central and midperipheral profound chorioretinal atrophy and coarse hyperpigmentation (Figures 2C, 2D), while others showed midperipheral patchy paving stone-like degeneration, and some patients maintaining a relatively spared posterior pole with only mild RPE alterations (Figures 2E, 2G, 2H). This considerable phenotypic variability in patients originating from the same genetic isolate and carrying the same homozygous mutation points to the involvement of genetic and/or environmental modifiers. Certain *Rpe65* variants have been shown to modify the disease course in mouse models of RP and albinism,[62, 63] although no such variants were found in our study. Bone spicule-like pigmentation was absent in two patients (15%), and limited or sparsely scattered in three patients (23%; Fig. 2). Eight patients (62%) had distinct areas of depigmentation. This finding is in line with previous observations of no or minimal hyperpigmentation in phenotypes associated with *LRAT* and *RPE65* mutations,[21, 31, 49] and areas of hypo- or depigmentation.[20]

Retinal imaging, in line with visual function, showed relatively well-preserved outer retinas in two patients in their second and sixth decade of life, and marked retinal or chorioretinal degeneration in two patients in their seventh and eighth decades of life. Preservation of central retinal structure, including outer photoreceptor layers on SD-OCT has been reported before in a younger patient (27 years) with different *LRAT* mutations.[21] The long-term preservation of the outer retina in these patients, at least at the level of the fovea, is a favorable finding, as it has been demonstrated that a relatively preserved photoreceptor layer predicts a positive treatment response in patients with IRDs associated with mutations *RPE65* or *LRAT* receiving oral synthetic 9-cis-retinoid in a clinical trial.[61, 64]

As a systemic therapeutic trial targeting the retinoid cycle in human patients has grouped patients with *LRAT*- and *RPE65*-associated RP and LCA,[27] and the same systemic or novel cell-based therapeutic strategies have grouped *Lrat*(-/-) and *Rpe65*(-/-) mouse models together,[65, 66] understanding the comparability of these phenotypes is important. Comparable LCA phenotypes

have been found in *Rpe65*(-/-) and *Lrat*(-/-) mice.[67,68] Similarly in human patients, parallels between the phenotypes associated with *LRAT* and *RPE65* mutations have been suggested in previous case studies of *LRAT*-RDs.[21,22] *RPE65* mutations typically lead to severe retinal degeneration, presenting with severely reduced vision in the first year of life, nystagmus, and panretinal photoreceptor degeneration, leading to a diagnosis of LCA or early-onset severe retinal degeneration.[6, 9, 54, 69] However, cases of *RPE65*-RP and early-onset IRD with relatively preserved ambulatory vision into adolescence have also been described.[37, 47, 50, 52, 56] Distinctive fundus features include white dots, just like we observed in six (46%) of the *LRAT*-RD patients in the current cohort, sometimes fading with time as also observed in one patient in the current study.[35, 46, 52] In RPE65-associated IRD, these white-yellow dots have also been described in fundus albipunctatus.[59,60] SD-OCT scans in several patients with *RPE65*-LCA have shown preserved retinal thickness and foveal contour, and attenuated but detectable outer photoreceptor layers, even in cases of visual impairment.[9, 55, 70] However, lamellar disorganization and/or outer retinal and photoreceptor layer disintegration have also been found in *RPE65*-LCA, with differing reports on the relationship with age.[36, 40, 53] Our findings in this *LRAT*-RD population indicate similarities with the retinal phenotype of *RPE65*-RDs, although the exceptionally extended period of retinal structural and functional preservation in the genetic isolate is distinct. Moreover, the findings in our study are variable, complicating the ability to make a clear comparison between phenotypes associated with mutations in *LRAT* and those associated with mutations in *RPE65*.

The drawbacks of this study include its retrospective design, and the limited historical availability of imaging and all modalities of functional testing, as most tests were available only for a subset of patients. Although we have found a symptomatically and visually more severe phenotype in the patient with the homozygous c.326G>T mutation than in the patients from the genetic isolate with a homozygous c.12del mutation, a larger and more genetically heterogeneous cohort would have allowed for the exploration of genotype-phenotype correlations, subgroup analyses, and for a more comprehensive description of the phenotypic spectrum. As the current literature on phenotypes associated with bi-allelic mutations in *LRAT* is limited, the generalizability of our findings in this Dutch and Belgian cohort to the general population of patients with *LRAT*-RDs is uncertain.

In conclusion, our findings in patients with IRDs associated with *LRAT*-mutations due to the c.12del mutation or c.326G>T mutation indicate that *LRAT*-RDs may be particularly amenable to treatment. Not all pathogenic variants in *LRAT* lead to early severe visual dysfunction, and the window of therapeutic opportunity may be extended to later decades of life in some patients. While fundus phenotypes were heterogeneous within this genetic isolate, similarities can be found with the heterogeneous phenotypes associated with *RPE65*-mutations.

Acknowledgments

This study was performed as part of a collaboration within the European Reference Network for Rare Eye Diseases (ERN-EYE). ERN-EYE is co-funded by the Health Program of the European Union under the Framework Partnership Agreement #739543 – 'ERN-EYE' and co-funded by the Hôpitaux Universitaires de Strasbourg.

Supported by grants from Stichting Blindenhulp, Janivo Stichting (CJFB).

REFERENCES

1. Hartong DT, Berson EL, Dryja TP. Retinitis pigmentosa. Lancet 2006;368:1795-809.
2. Booij JC, Florijn RJ, ten Brink JB, et al. Identification of mutations in the AIPL1, CRB1, GUCY2D, RPE65, and RPGRIP1 genes in patients with juvenile retinitis pigmentosa. J Med Genet 2005;42:e67.
3. van Soest S, Westerveld A, de Jong PT, et al. Retinitis pigmentosa: defined from a molecular point of view. Surv Ophthalmol 1999;43:321-34.
4. Redmond TM, Yu S, Lee E, et al. Rpe65 is necessary for production of 11-cis-vitamin A in the retinal visual cycle. Nat Genet 1998;20:344-51.
5. Batten ML, Imanishi Y, Maeda T, et al. Lecithin-retinol acyltransferase is essential for accumulation of all-trans-retinyl esters in the eye and in the liver. J Biol Chem 2004;279:10422-32.
6. den Hollander AI, Roepman R, Koenekoop RK, Cremers FPM. Leber congenital amaurosis: Genes, proteins and disease mechanisms. Prog Ret Eye Res 2008;27:391-419.
7. Hanein S, Perrault I, Gerber S, et al. Leber congenital amaurosis: comprehensive survey of the genetic heterogeneity, refinement of the clinical definition, and genotype-phenotype correlations as a strategy for molecular diagnosis. Hum Mutat 2004;23:306-17.
8. Bramall AN, Wright AF, Jacobson SG, McInnes RR. The genomic, biochemical, and cellular responses of the retina in inherited photoreceptor degenerations and prospects for the treatment of these disorders. Annu Rev Neurosci 2010;33:441-72.
9. Simonelli F, Ziviello C, Testa F, et al. Clinical and molecular genetics of Leber's congenital amaurosis: a multicenter study of Italian patients. Invest Ophthalmol Vis Sci 2007;48:4284-90.
10. Katagiri S, Hayashi T, Kondo M, et al. RPE65 Mutations in Two Japanese Families with Leber Congenital Amaurosis. Ophthalmic Genet 2016;37:161-9.
11. Srilekha S, Arokiasamy T, Srikrupa NN, et al. Homozygosity Mapping in Leber Congenital Amaurosis and Autosomal Recessive Retinitis Pigmentosa in South Indian Families. PLoS One 2015;10:e0131679.
12. Jakobsson C, Othman IS, Munier FL, et al. Cone-rod dystrophy caused by a novel homozygous RPE65 mutation in Leber congenital amaurosis. Klin Monbl Augenheilkd 2014;231:405-10.
13. Chen Y, Zhang Q, Shen T, et al. Comprehensive mutation analysis by whole-exome sequencing in 41 Chinese families with Leber congenital amaurosis. Invest Ophthalmol Vis Sci 2013;54:4351-7.
14. Roman AJ, Cideciyan AV, Schwartz SB, et al. Intervisit variability of visual parameters in Leber congenital amaurosis caused by RPE65 mutations. Invest Ophthalmol Vis Sci 2013;54:1378-83.
15. McKibbin M, Ali M, Mohamed MD, et al. Genotype-phenotype correlation for leber congenital amaurosis in Northern Pakistan. Arch Ophthalmol 2010;128:107-13.
16. Hull S, Mukherjee R, Holder GE, et al. The clinical features of retinal disease due to a dominant mutation in RPE65. Mol Vis 2016;22:626-35.
17. Bowne SJ, Humphries MM, Sullivan LS, et al. A dominant mutation in RPE65 identified by whole-exome sequencing causes retinitis pigmentosa with choroidal involvement. Eur J Hum Genet 2011;19:1074-81.
18. Jauregui R, Park KS, Tsang SH. Two-year progression analysis of RPE65 autosomal dominant retinitis pigmentosa. Ophthalmic Genet 2018;39:544-9.

19. Thompson DA, Li Y, McHenry CL, et al. Mutations in the gene encoding lecithin retinol acyltransferase are associated with early-onset severe retinal dystrophy. Nat Genet 2001;28:123-4.
20. den Hollander AI, Lopez I, Yzer S, et al. Identification of novel mutations in patients with Leber congenital amaurosis and juvenile RP by genome-wide homozygosity mapping with SNP microarrays. Invest Ophthalmol Vis Sci 2007;48:5690-8.
21. Dev Borman A, Ocaka LA, Mackay DS, et al. Early onset retinal dystrophy due to mutations in LRAT: molecular analysis and detailed phenotypic study. Invest Ophthalmol Vis Sci 2012;53:3927-38.
22. Senechal A, Humbert G, Surget MO, et al. Screening genes of the retinoid metabolism: novel LRAT mutation in leber congenital amaurosis. Am J Ophthalmol 2006;142:702-4.
23. Preising MN, Paunescu K, Friedburg C, Lorenz B. Genetic and clinical heterogeneity in LCA patients. The end of uniformity [in German]. Ophthalmologe 2007;104:490-8.
24. Maguire AM, Simonelli F, Pierce EA, et al. Safety and Efficacy of Gene Transfer for Leber's Congenital Amaurosis. N Engl J Med 2008;358:2240-8.
25. Bennett J, Wellman J, Marshall KA, et al. Safety and durability of effect of contralateral-eye administration of AAV2 gene therapy in patients with childhood-onset blindness caused by RPE65 mutations: a follow-on phase 1 trial. Lancet 2016;388:661-72.
26. FDA approves novel gene therapy to treat patients with a rare form of inherited vision loss. U.S. Food and Drug Administration, 2017. Available at: https://www.fda.gov/newsevents/newsroom/pressannouncements/ucm589467.htm. Accessed April 2, 2019.
27. Koenekoop RK, Sui R, Sallum J, et al. Oral 9-cis retinoid for childhood blindness due to Leber congenital amaurosis caused by RPE65 or LRAT mutations: an open-label phase 1b trial. Lancet 2014;384:1513-20.
28. Littink KW, van Genderen MM, van Schooneveld MJ, et al. A homozygous frameshift mutation in LRAT causes retinitis punctata albescens. Ophthalmology 2012;119:1899-906.
29. Mathijssen IB, Florijn RJ, van den Born LI, et al. Long-term follow-up of patients with retinitis pigmentosa type 12 caused by CRB1 mutations: A Severe Phenotype With Considerable Interindividual Variability. Retina 2017;37:161-172.
30. Talib M, van Schooneveld MJ, van Genderen MM, et al. Genotypic and Phenotypic Characteristics of CRB1-Associated Retinal Dystrophies: A Long-Term Follow-up Study. Ophthalmology 2017;124:884-95.
31. Coppieters F, Van Schil K, Bauwens M, et al. Identity-by-descent-guided mutation analysis and exome sequencing in consanguineous families reveals unusual clinical and molecular findings in retinal dystrophy. Genet Med 2014;16:671-80.
32. McCulloch DL, Marmor MF, Brigell MG, et al. ISCEV Standard for full-field clinical electroretinography (2015 update). Doc Ophthalmol 2015;130:1-12.
33. Dagnelie G. Conversion of planimetric visual field data into solid angles and retinal areas. Clin Vis Sci 1990;5:95-100.
34. Biswas P, Duncan JL, Maranhao B, et al. Genetic analysis of 10 pedigrees with inherited retinal degeneration by exome sequencing and phenotype-genotype association. Physiol Genomics 2017;49:216-29.
35. Xu F, Dong Q, Liu L, et al. Novel RPE65 mutations associated with Leber congenital amaurosis in Chinese patients. Mol Vis 2012;18:744-50.

36. Pasadhika S, Fishman GA, Stone EM, et al. Differential macular morphology in patients with RPE65-, CEP290-, GUCY2D-, and AIPL1-related Leber congenital amaurosis. Invest Ophthalmol Vis Sci 2010;51:2608-14.
37. Walia S, Fishman GA, Jacobson SG, et al. Visual acuity in patients with Leber's congenital amaurosis and early childhood-onset retinitis pigmentosa. Ophthalmology 2010;117:1190-8.
38. Li Y, Wang H, Peng J, et al. Mutation survey of known LCA genes and loci in the Saudi Arabian population. Invest Ophthalmol Vis Sci 2009;50:1336-43.
39. Jacobson SG, Aleman TS, Cideciyan AV, et al. Identifying photoreceptors in blind eyes caused by RPE65 mutations: Prerequisite for human gene therapy success. Proc Natl Acad Sci U S A 2005;102:6177-82.
40. Jacobson SG, Cideciyan AV, Aleman TS, et al. Photoreceptor Layer Topography in Children with Leber Congenital Amaurosis Caused by RPE65 Mutations. Invest Ophthalmol Vis Sci 2008;49:4573-7.
41. Galvin JA, Fishman GA, Stone EM, Koenekoop RK. Evaluation of genotype-phenotype associations in leber congenital amaurosis. Retina 2005;25:919-29.
42. Silva E, Dharmaraj S, Li YY, et al. A missense mutation in GUCY2D acts as a genetic modifier in RPE65-related Leber Congenital Amaurosis. Ophthalmic Genet 2004;25:205-17.
43. Sitorus RS, Lorenz B, Preising MN. Analysis of three genes in Leber congenital amaurosis in Indonesian patients. Vision Res 2003;43:3087-93.
44. Hamel CP, Griffoin JM, Lasquellec L, et al. Retinal dystrophies caused by mutations in RPE65: assessment of visual functions. Br J Ophthalmol 2001;85:424-7.
45. Dharmaraj SR, Silva ER, Pina AL, et al. Mutational analysis and clinical correlation in Leber congenital amaurosis. Ophthalmic Genet 2000;21:135-50.
46. Chebil A, Falfoul Y, Habibi I, et al. [Genotype-phenotype correlation in ten Tunisian families with non-syndromic retinitis pigmentosa]. J Fr Ophtalmol 2016;39:277-86.
47. Morimura H, Fishman GA, Grover SA, et al. Mutations in the RPE65 gene in patients with autosomal recessive retinitis pigmentosa or leber congenital amaurosis. Proc Natl Acad Sci U S A 1998;95:3088-93.
48. Kabir F, Naz S, Riazuddin SA, et al. Novel mutations in RPE65 identified in consanguineous Pakistani families with retinal dystrophy. Mol Vis 2013;19:1554-64.
49. El Matri L, Ambresin A, Schorderet DF, et al. Phenotype of three consanguineous Tunisian families with early-onset retinal degeneration caused by an R91W homozygous mutation in the RPE65 gene. Graefes Arch Clin Exp Ophthalmol 2006;244:1104-12.
50. Thompson DA, Gyurus P, Fleischer LL, et al. Genetics and phenotypes of RPE65 mutations in inherited retinal degeneration. Invest Ophthalmol Vis Sci 2000;41:4293-9.
51. Mo G, Ding Q, Chen Z, et al. A novel mutation in the RPE65 gene causing Leber congenital amaurosis and its transcriptional expression in vitro. PLoS One 2014;9:e112400.
52. Weleber RG, Michaelides M, Trzupek KM, et al. The phenotype of Severe Early Childhood Onset Retinal Dystrophy (SECORD) from mutation of RPE65 and differentiation from Leber congenital amaurosis. Invest Ophthalmol Vis Sci 2011;52:292-302.
53. Lorenz B, Poliakov E, Schambeck M, et al. A comprehensive clinical and biochemical functional study of a novel RPE65 hypomorphic mutation. Invest Ophthalmol Vis Sci 2008;49:5235-42.

54. Paunescu K, Wabbels B, Preising MN, Lorenz B. Longitudinal and cross-sectional study of patients with early-onset severe retinal dystrophy associated with RPE65 mutations. Graefe's Archive for Clinical and Experimental Ophthalmology 2005;243:417-26.
55. Lorenz B, Wabbels B, Wegscheider E, et al. Lack of fundus autofluorescence to 488 nanometers from childhood on in patients with early-onset severe retinal dystrophy associated with mutations in RPE65. Ophthalmology 2004;111:1585-94.
56. Yzer S, van den Born LI, Schuil J, et al. A Tyr368His RPE65 founder mutation is associated with variable expression and progression of early onset retinal dystrophy in 10 families of a genetically isolated population. J Med Genet 2003;40:709-13.
57. Felius J, Thompson DA, Khan NW, et al. Clinical course and visual function in a family with mutations in the RPE65 gene. Arch Ophthalmol 2002;120:55-61.
58. Katagiri S, Hosono K, Hayashi T, et al. Early onset flecked retinal dystrophy associated with new compound heterozygous RPE65 variants. Mol Vis 2018;24:286-96.
59. Yang G, Liu Z, Xie S, et al. Genetic and phenotypic characteristics of four Chinese families with fundus albipunctatus. Sci Rep 2017;7:46285.
60. Schatz P, Preising M, Lorenz B, et al. Fundus albipunctatus associated with compound heterozygous mutations in RPE65. Ophthalmology 2011;118:888-94.
61. Scholl HP, Moore AT, Koenekoop RK, et al. Safety and Proof-of-Concept Study of Oral QLT091001 in Retinitis Pigmentosa Due to Inherited Deficiencies of Retinal Pigment Epithelial 65 Protein (RPE65) or Lecithin:Retinol Acyltransferase (LRAT). PLoS One 2015;10:e0143846.
62. Samardzija M, Wenzel A, Naash M, et al. Rpe65 as a modifier gene for inherited retinal degeneration. Eur J Neurosci 2006;23:1028-34.
63. Danciger M, Matthes MT, Yasamura D, et al. A QTL on distal chromosome 3 that influences the severity of light-induced damage to mouse photoreceptors. Mamm Genome 2000;11:422-7.
64. Wen Y, Birch DG. Outer Segment Thickness Predicts Visual Field Response to QLT091001 in Patients with RPE65 or LRAT Mutations. Transl Vis Sci Technol 2015;4:8.
65. Maeda T, Lee MJ, Palczewska G, et al. Retinal pigmented epithelial cells obtained from human induced pluripotent stem cells possess functional visual cycle enzymes in vitro and in vivo. J Biol Chem 2013;288:34484-93.
66. Maeda T, Dong Z, Jin H, et al. QLT091001, a 9-cis-retinal analog, is well-tolerated by retinas of mice with impaired visual cycles. Invest Ophthalmol Vis Sci 2013;54:455-66.
67. Fan J, Rohrer B, Frederick JM, et al. Rpe65-/- and Lrat-/- mice: comparable models of leber congenital amaurosis. Invest Ophthalmol Vis Sci 2008;49:2384-9.
68. Zhang H, Fan J, Li S, et al. Trafficking of membrane-associated proteins to cone photoreceptor outer segments requires the chromophore 11-cis-retinal. J Neurosci 2008;28:4008-14.
69. Gu SM, Thompson DA, Srikumari CR, et al. Mutations in RPE65 cause autosomal recessive childhood-onset severe retinal dystrophy. Nat Genet 1997;17:194-7.
70. Van Hooser JP, Aleman TS, He YG, et al. Rapid restoration of visual pigment and function with oral retinoid in a mouse model of childhood blindness. Proc Natl Acad Sci U S A 2000;97:8623-8.

SUPPLEMENTAL MATERIAL

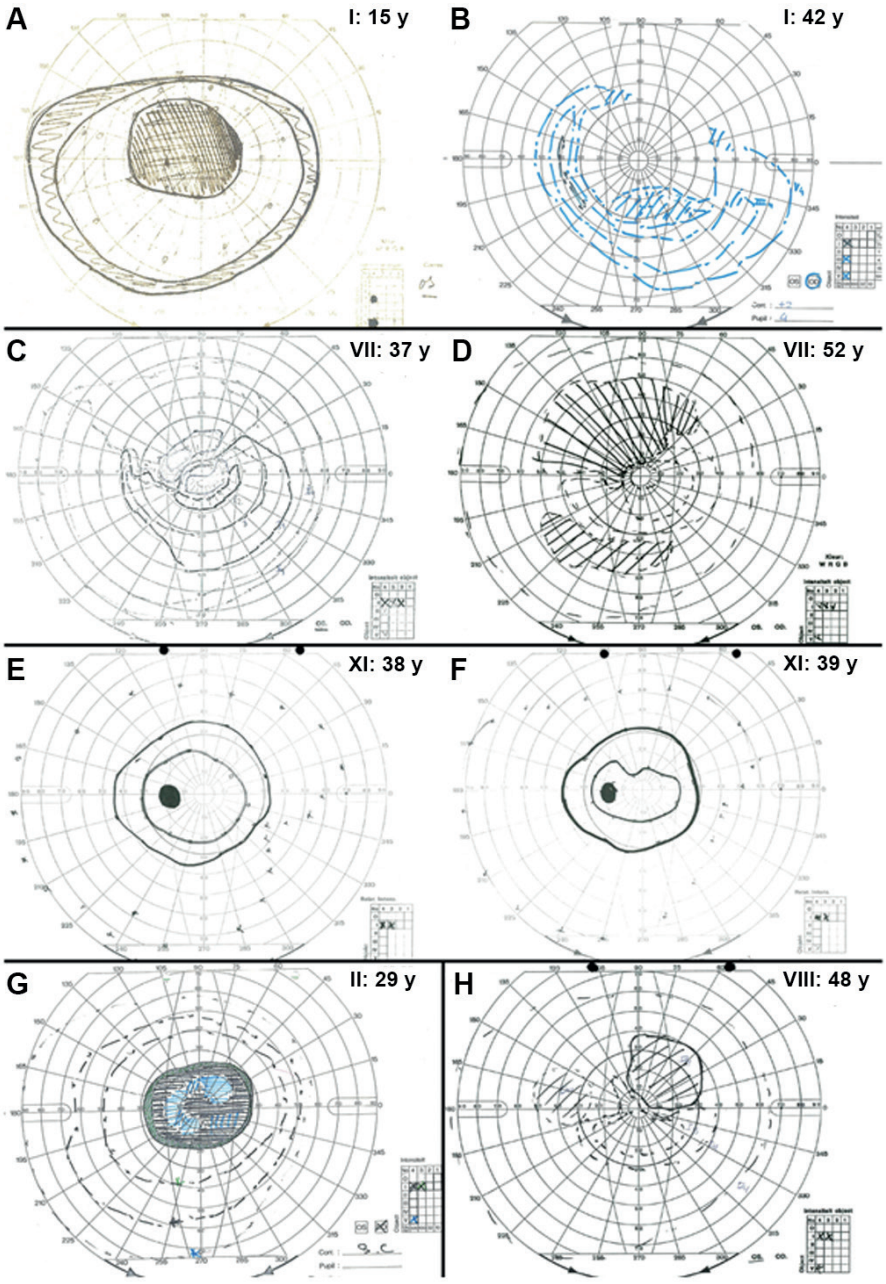

Supplementary Figure S1. Goldmann visual fields in patients retinal degeneration associated with mutations in *LRAT*. Shaded areas represent scotomas. **A-B.** Progression of the visual field defects in patient I between the ages

of 15 (**A**) and 42 (**B**) years. This patient had nondetectable rod or cone responses on electroretinography, but his sibling, patient II, was diagnosed with *LRAT*-associated cone-rod degeneration based on his electroretinogram. **C-D.** Progression of the visual field defects in patient VII, who was diagnosed with retinitis pigmentosa (RP), between the ages 37 (**C**) and 52 (**D**) years. **E-F.** Patient XI, who had RP, showing relative concentric constriction of the smaller (I4e) targets, with a relatively well-preserved V4e isopter size between the ages of 38 (**E**) and 39 (**F**) years. **G.** Patient II, a cone-rod degeneration patient, at the age of 29 years, showing an absolute central scotoma, with a sensitivity reduction in the fovea. **H.** Patient VIII, who had RP, at the age of 48, showing relative concentric constriction, and an absolute midperipheral scotoma encroaching on the fovea.

Supplementary Table S1. Visual fields in patients with retinal degeneration associated with mutations in *LRAT*

ID	Age[a] (y)	Central horizontal diameter V-4e (°)		Central horizontal diameter I-4e (°)		Min. seen[b]	Seeing retinal area V4e (mm^2)			Pattern
		OD	OS	OD	OS		OD	OS	Change (mm^2/year)	
I	50	0	0	0	0	I-4e	213.6	234.6	-16.8	Absolute central scotoma. Peripheral wedge of vision.
	23	1.5	2	0	0	III-4e	NA†	679.1		Large absolute central scotoma with small island of foveal sparing. Midperipheral remaining ring.
II	29	73	63	0	0	I-3e	768.3	725.7		Relative central scotoma (≤I4e). Absolute paracentral scotoma.
III	30	NA†		NA†		NA†	NA†			Supra-temporal absolute scotoma; relative central scotoma
VII	52	72	66	39-10	55	I-2e	543.9	543.5	-15.4	Midperipheral absolute scotomas, encroaching towards fovea. Relative concentric constriction.
	37	145	142	48-10	53	I-2e	782.8	765.7		Relative paracentral scotomas. Relative concentric constriction, mainly superior hemifield.
VIII	48	153	98	30-3	11	I-3e	707.1	691.9		Absolute midperipheral and paracentral scotomas.
IX	11	NA[c]		NA[c]		NA[c]	NA[c]			Multiple relative scotomas in periphery.
X	40	NA[c]		NA[c]		NA[c]	NA[c]			Absolute concentric constriction, 20° from fovea
XI	39	130	140	73	70	I-3e	700.6	716.2	-13.4	Absolute concentric constriction.
	38	140	150	75	77	I-3e	718.9	736.2		Absolute concentric constriction.
XII	54	NA[d]		NA[d]		NA[d]	NA[d]			Absolute scotoma encroaching upon 10° from fovea.

	17	134	123	0	3	II4e/ I4e	562.5	530.0	+41.9	Absolute concentric constriction.
XIII	16	116	128	0	2	II4e/ I4e	455.6	507.2		Increased concentric constriction.
	15	116	130	4	2	I4e	452.2	512.0		Absolute concentric constriction.

NA, not available.

The horizontal diameter, as measured from the vertical meridian, uninterrupted by scotomas, was used to determine the central visual field. When a paracentral scotoma interrupted the horizontal meridian, this was considered the border as measured from the center..

[a] Age at the moment of the examination with Goldmann kinetic perimetry.

[b] Minimal isopter size observed on Goldmann kinetic perimetry.

[c] No Goldmann visual field output available, only a description of the visual field in the medical record.

[d] No Goldmann visual field, but a different perimetry modality (Humphrey 30-2 perimetry).